Human Serum Albumin binding Ibuprofen: A 3D description of the unfolding pathway in urea

Luciano Galantini, Claudia Leggio, Peter V. Konarev, Nicolae V. Pavel

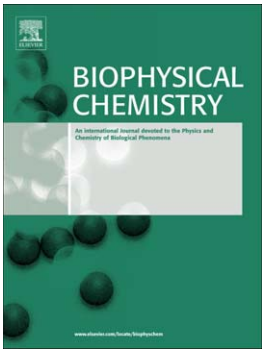

Human Serum Albumin binding Ibuprofen: A 3D description of the unfolding pathway in urea

Luciano Galantini, Claudia Leggio, Peter V. Konarev, Nicolae V. Pavel

PII: S0301-4622(10)00003-7
DOI: doi: 10.1016/j.bpc.2010.01.002
Reference: BIOCHE 5332

To appear in: *Biophysical Chemistry*

Received date: 9 November 2009
Revised date: 8 January 2010
Accepted date: 10 January 2010

Please cite this article as: Luciano Galantini, Claudia Leggio, Peter V. Konarev, Nicolae V. Pavel, Human Serum Albumin binding Ibuprofen: A 3D description of the unfolding pathway in urea, *Biophysical Chemistry* (2010), doi: 10.1016/j.bpc.2010.01.002

Human Serum Albumin binding Ibuprofen: a 3D description of the unfolding pathway in urea.

Luciano Galantini[a], *Claudia Leggio*[a,*], *Peter V. Konarev*[b], *and Nicolae V. Pavel*[a]

[a] Dipartimento di Chimica, Sapienza Università di Roma, P.O. Box 34-Roma 62, Piazzale A. Moro 5, I-00185 Roma, Italy, and INFM CRS-SOFT, c/o Sapienza Università di Roma, Roma, Italy

[b] European Molecular Biology Laboratory, Hamburg Outstation, D-22603 Hamburg, Germany.

E-mail addresses of the authors: l.galantini@caspur.it, c.leggio@caspur.it, konarev@EMBL-Hamburg.de, v.pavel@caspur.it

[*] To whom correspondence should be addressed: Claudia Leggio, Dipartimento di Chimica, Sapienza Università di Roma, P.O. Box 34-Roma 62, P.le A. Moro 5, I-00185 Rome, Italy; telephone +39 06 4991 3714, fax +39 06 490631; e-mail: c.leggio@caspur.it

Abstract

Small angle X-ray scattering (SAXS) technique, supported by light scattering measurements and spectroscopic data (circular dichroism and fluorescence) allowed us to restore the 3D structure at low resolution of defatted human serum albumin (HSA) in interaction with ibuprofen. The data were carried out on a set of HSA solutions with urea concentrations between 0.00 and 9.00 M. The Singular Value Decomposition method, applied to the complete SAXS data set allowed us to distinguish three different states in solution. In particular a native conformation N (at 0.00 M urea), an intermediate I1 (at 6.05 M urea) and an unfolded structure U (at 9.00 M urea) were recognized. The low resolution structures of these states were obtained by exploiting both *ab initio* and rigid body fitting methods. In particular, for the protein without denaturant, a conformation recently described (Leggio & al., PCCP, 2008, 10, 6741-6750), very similar to the crystallographic heart shape, with only a slight reciprocal movement of the three domains, was confirmed. The I1 structure was instead characterized by only a closed domain (domain III) and finally, the recovered structure of the U state revealed the characteristic feature of a completely open state. A direct comparison with the free HSA pointed out that the presence of the ibuprofen provokes a shift of the equilibrium towards higher urea concentrations without changing the unfolding sequence. The work represents a type of analysis which could be exploited in future investigations on proteins in solution, in the binding of drugs or endogenous compounds and in the pharmacokinetic properties as well as in the study of allosteric effects, cooperation or anticooperation mechanisms.

Introduction

Human Serum Albumin (HSA), the most prominent protein in plasma, is best known for its extraordinary capacity of binding a wide variety of compounds that may be available in quantities well beyond their solubility in plasma. For example, albumin is the main transport vehicle for fatty acids (FA) to and from the tissues, by increasing their effective solubility from < 1μM to millimolar values.[1] The high concentration in the circulatory system (about 42 g/L) and the capability to store a big amount of drugs, metabolites and fatty acids assign to the HSA a really important role in the pharmacokinetic behavior of many compounds, affecting their efficacy and delivery rate.

Many studies on the HSA binding properties[2-7] have shown that the hydrophobic subdomains IIA and IIIA represent the principal binding regions on HSA.

According to the Sudlow's nomenclature, dicarboxylic acids and/or bulky heterocyclic molecules with a negative charge localized in the middle of the molecule, bind to Sudlow's site I (located in subdomain IIA). The site must be large because ligands as big as bilirubin can be bound, and because several examples of independent binding of two different compounds to the site have been found.[8-11] Sudlow's site II (located in subdomain IIIA) is preferred by aromatic carboxylic acids with a negatively charged acidic group at one end of the molecule away from a hydrophobic center (e.g., non-steroidal anti-inflammatory drugs). Site II is composed of all six helices of subdomain IIIA and it is topologically similar to site I but it seems to be smaller, or more narrow, than site I, because apparently no large ligands (e.g., bilirubin, hemin, hematin, or other porphyrins) bind to it. It also appears to be less flexible, because binding often is strongly affected by stereoselectivity. For example the ibuprofen, a chiral nonsteroidal anti-inflammatory agent, considered as stereotypical ligand for Sudlow's site II, presents an affinity that is 2.3 times bigger for the R-ibuprofen than for S-ibuprofen.[12,13]

Besides the two principal binding sites there is a multiplicity of different points of attack for the fatty acids and other drugs, that can also be controlled by allosteric conformational changes.[14] Among

the exogenous and endogenous compounds which bind the albumin, it is very interesting to classify the drugs that protect the protein against the denaturation. Within the wide variety of substances that had been studied, a particular attention is focused on the nonsteroidal anti-inflammatory drugs (NSAIDs). So far, essentially turbidimetric and HPLC measurements have been carried out to understand and to quantify the stabilization properties of various compounds. Saso et al.[15,16] reported the stabilization activity of numerous drugs, studying the variation of absorbance (turbidimetric method) or the aggregation (HPLC technique) of HSA:ligand solutions in heat-induced denaturation conditions. These works show that FA, NSAIDs and a surfactant, the sodium dodecyl sulfate, are the more active compounds.

A recent fast-field-cycling 1H-NMR relaxometric study[17] shows that, in both urea- and GdnHCl-induced unfolding processes, the anti-inflammatory drug ibuprofen is able to dramatically stabilize the Normal isomer of the heme-HSA. Moreover, it has been proposed that the unfolding of domain I always follows the unfolding of domain II.[18,19] Although ibuprofen is a stereotypical Sudlow's site II ligand, it also binds to a cleft close to the warfarin site at the interface between subdomains IIA and IIB.[20]

The main aim of this work was to investigate the influence of the ibuprofen on the urea-induced denaturation of the protein and to point out its possible stabilizing activity. We performed a study on the HSA:ibuprofen complex at various urea concentrations and we compared it with the free HSA denaturation in the same conditions.[21] The comparison, besides establishing the ibuprofen stabilization activity, can help us in the definition of the domain opening sequence in the structure reconstruction, thus further clarifying the albumin unfolding mechanism.

Experimental section

Sample preparation

Delipidated human serum albumin (>96 %, type A1887), obtained from Sigma, was dissolved in 10 mM phosphate buffer at pH 7.2 with the addition of 11 mM sodium azide. The albumin was magnetically gently stirred for about 12 hours and then filtered with a nucleopore filter with a diameter of 100 nm. Ibuprofen, type I1892 purchased from Sigma, dissolved in phosphate buffer at pH 7.2, was added to the HSA solution, before the denaturant agent, with a stechiometric ratio ligand:HSA 10:1 (HSAIbu). After about 5 hours, HSAIbu samples with urea, obtained from Riedel-Hahn, were prepared by adding the solid denaturant agent to the solutions. After about 10 hours the solutions were filtered again (diameter of 30 nm) and were analyzed in less than a week.

For the fluorescence and circular dichroism (CD) measurements the HSA concentration was less than 1g/L (15 µM). For the dynamic light scattering (DLS) and Small angle X-ray scattering (SAXS) measurements, the protein concentration reached 4 g/L (60 µM). Protein concentration was determined spectrophotometrically using ε_{280} = 35700 $M^{-1}cm^{-1}$.[22] Bidistilled water was used in the preparation of buffer. All experiments were conducted at room temperature (25 °C).

Spectroscopic measurements

The absorbance measurements were performed with a Cary 1E UV-VIS spectrophotometer and a Thermo Scientific NanoDrop 1000 UV-VIS spectrophotometer. Unfolding of the protein was monitored both by fluorescence and CD techniques. The fluorescence studies were performed using a Cary Eclipse spectrofluorometer. A quartz cuvette of 1 cm path length was used and the intrinsic fluorescence was measured by exciting the protein solution at λ_{ex}= 280 and 295 nm with a band-pass of both excitation and emission monochromators of 5 nm. The CD spectra (four averaged acquisitions) were recorded in a JASCO J-750 spectropolarimeter at 25 °C using a bandwidth of 2 nm. A 0.1 mm

path length was used for the far-UV spectra and a 10 mm cuvette was used for the near-UV region. The secondary structure was monitored by calculating with the equation proposed by Chen[23] the percentage of α-helix considering the value of the Mean Residue Ellipticity (MRE) at 222 nm (deg cm^2 $dmol^{-1}$).

DLS measurements

In the DLS experiments, the intensity-intensity autocorrelation function is measured and related to the normalized electric field autocorrelation function $g_1(\tau)$ by the Siegert relation. The $g_1(\tau)$ analysis through the cumulant expansion, allows the determination of the so called apparent diffusion coefficient D_{app}, from the first cumulant value. For very diluted samples (no particle interactions), the hydrodynamic radius R_h of the scattering particle can be calculated from the D_{app} value, by the Stokes Einstein equation. Moreover, a $g_1(\tau)$ analysis by CONTIN can be performed to verify multimodal distributions of the particle sizes. This confirms that the protein remains monomeric in solution under the experimental conditions used for carrying out the SAXS experiments.

The measurements were performed using a Brookhaven instrument constituted by a BI-2030AT digital correlator with 136 channels, and a BI-200SM goniometer. The light source was a Uniphase solid-state laser system model 4601 operating at 532 nm. The solutions were filtered by means of a Brookhaven ultrafiltration unit (BIUU1) for flow-through cells, the volume of the flow cell being about 1.0 cm^3. The samples were placed in the cell for at least 30 min prior the measurement to permit the thermal equilibration. Their temperature was kept constant within 0.5 °C by a circulating water bath. Measures performed in the range 30°-150° showed that the data were not affected by the collecting angle. The reported data refer to a scattering angle of 90°.

SAXS measurements

SAXS data were collected at the X33 beam line of the European Molecular Biology Laboratory (EMBL), Hamburg outstation at the storage ring DORIS III of the Deutsches Elektronen Synchrotron (DESY) synchrotron[24] and analyzed according to standard procedures.[25] Solutions with protein concentrations from 1.0 to 3.0 mg/ml were measured at 25 °C for 3 min exposure time on an image plate detector (MAR345; MarResearch, Norderstedt, Germany). The sample-detector distance of 2.4 m covered the range of momentum transfer $0.01 < q < 0.45$ Å^{-1} ($q=4\pi \sin(\theta)/\lambda$, where 2θ is the scattering angle and λ = 0.15 nm is the X-ray wavelength). Repetitive exposures of the same protein solution indicated no changes in the scattering patterns, i.e., no measurable radiation damage of the protein samples. The data were normalized to the intensity of the transmitted beam and the scattering of the buffer was subtracted. All the data processing steps were performed with the program package PRIMUS.[26] The molecular mass of each sample was estimated by comparing the extrapolated forward scattering *I(0)* with that of a reference solution made of human serum albumin at pH 7.2.

In house SAXS measurements were carried out in thermostatted (25.0 ± 0.1 °C) quartz capillary of 1 mm by using a Kratky compact camera, containing a slit collimation system, equipped with a NaI scintillation counter. Ni-filtered Cu Kα radiation (λ=1.5418 Å) was used. Scattering curves were recorded within the range $0.01 < q < 0.5$ Å^{-1}. The moving slit method was employed to measure the intensity of the primary beam. The collimated scattering intensities were put on an absolute scale, subtracted for the solvent and the capillary contributions, and then expressed in electron units, eu (electrons^2 Å^{-3}) per centimeter primary-beam length.[27,28] In terms of total scattering cross section of an ensemble of particles, 1 eu corresponds to $7.94056 \cdot 10^{-2}$ cm^{-1}.[29]

The Indirect Fourier Transform method developed in the ITP program was used for interpreting the spectra.[30] For very dilute samples (no particle interactions) the scattered intensity, *I(q)*, can be related to the pair distribution function *p(r)* of the single scattering particle according with the equation

$$I(q) = \int_0^{\infty} p(r)\frac{\sin(qr)}{qr}dr \qquad (1)$$

On the basis of this equation, the Indirect Fourier Transform Method, allows the extraction of the *p(r)* function from the desmeared scattering pattern. The *p(r)* function is strongly dependent on the shape and size of the scattering particles and vanishes at the maximum particle size D_{max}. Furthermore, it permits the determination of the electronic radius of gyration R_g.[30]

2.5 Singular Value Decomposition

We employed the Singular Value Decomposition (SVD) method to determine the minimum number of structural states present in the HSAIbu unfolding process. The method is based on a theorem of linear algebra for which any M x N matrix A (with M ≥ N) can be written as the product of a column-orthogonal matrix U, an N x N diagonal matrix with non-negative elements (w_j) called single values, and the transpose of an N x N orthogonal matrix V.[31]

$$A=UWV^T \qquad (2)$$

Each column of the matrix A is constructed entering the N $I(q)q^2$ profiles (each corresponding to one of the N urea solutions). According to the SVD analysis, the entire set of scattering curves (with a number of scattering vectors *q* equal to M) can be represented by the product of a complete set of bases (orthogonal matrix U) and the correspondent weight (WV^T). In this way any scattering pattern, corresponding to a *t* urea concentration can be approximated:

$$I(q,t) = \sum_{j=1}^{L} u_j(q) w_j v_j(t) = \sum_{j=1}^{L} u_j(q) b_j(t) \qquad (3)$$

where *L* represents the minimum number of the bases *u* necessary to adequately reproduce the complete set of scattering intensities and the $b_j(t)$ is the *j*th basis coefficient at the urea concentration *t*.[32]

In particular, for L=3, since the scattering intensity is additive, any $I(q,t)$ (and also any $I(q)q^2$ profile) can be expressed as:

$$I(q,t)q^2 = f_N(t)I_N(t)q^2 + f_I(t)I_I(t)q^2 + f_U(t)I_U(t)q^2 \quad (4)$$

where the suffixes N, I and U indicate the Native, the Intermediate and the Unfolded states, respectively and $f_N(t)+f_I(t)+f_U(t)=1$. By applying the Equation 3 we can calculate the $b_j(t)$ coefficients

$$b_{1,calc} = f_N(t)b_{1,N} + f_I(t)b_{1,I} + f_U(t)b_{1,U} \quad (5a)$$

$$b_{2,calc} = f_N(t)b_{2,N} + f_I(t)b_{2,I} + f_U(t)b_{2,U} \quad (5b)$$

$$b_{3,calc} = f_N(t)b_{3,N} + f_I(t)b_{3,I} + f_U(t)b_{3,U} \quad (5c)$$

The $b_{j,I}$ and the Native, Intermediate and Unfolded fractions at each t urea concentration could be evaluated minimizing the equation

$$\chi^2 = \sum_{t=1}^{N}\sum_{j=1}^{L}\left(b_j(t) - b_{j,calc}(t)\right)^2 \quad (6)$$

In the case of a two states process (L=2) only the Native and the Unfolded forms are present and the percentage of Native form at each t urea concentration could be estimated as

$$f_N(t) = \frac{b_j(t) - b_{j,U}}{b_{j,N} - b_{j,U}} = \frac{X(t) - X_U}{X_N - X_U} \quad (7)$$

This function, in a single step mechanism, can be applied to several parameters that own the additive property (X) as: R_g^2, R_h^{-1}, mean residue ellipticity at 222 nm and at 268 nm (MRE_{222}, MRE_{268}) and fluorescence intensity at λ_{ex}= 280 nm and λ_{em}= 340 nm ($F340_{280}$).

For a three step process, the ratio $(X(t)-X_U)/(X_N-X_U)$ does not represent the $f_N(t)$ function and, for this reason, a different trend of this ratio, for the various parameters, could be an evidence of the presence in solution of at least an intermediate.

The equations 3-6 can be also applied to the curves obtained by other techniques (for example CD and fluorescence). A different value of the minimum number of structural states present in the unfolding process can be due or to an unlike denaturation mechanism (the loss of the secondary structure can be different from the tertiary one) or to a less resolution properties (for example the near-CD vs. the SAXS spectra).

2.6 Three-dimensional restored structures

Thanks to modern methods of data analysis, low-resolution 3D electron density maps from 1D SAXS data can be reliably reconstructed. Two complementary methods, developed in the programs GA_STRUCT and BUNCH, were used to obtain 3D structural information on the partially unfolded conformations that albumin presents in denaturant conditions.

The shape reconstruction method applied in the GA_STRUCT code is described in detail in the reference 33. Briefly, starting from an aggregate of spheres, related to the expected volume and the D_{max} of the scattering particle, the *p(r)* is calculated by means of a Monte Carlo method. A fitting parameter is determined from the calculated (Fourier transform) *I(q)* and the experimental one. A linear minimization is performed using a genetic algorithm which improves 50 models by means of mating, mutation and extinction operations. At the end, all models are docked and on the basis of a docking score, from the 70% of models with the highest total docking score a consensus envelope is constructed. It is important to stress that the volume of the consensus envelope constitutes an index of the conformational flexibility. As a matter of fact, in the case of a particle which presents a degree of conformational flexibility, this volume is correlated with the spatial region ensemble occupied by more similar models as shape and dimension. Therefore, its value will increase, exceeding the expected volume of a single frozen conformation.[34]

The analysis of the SAXS intensity profiles may use more information such as high resolution structures of whole domains or fragments and plausible hypothesis on the position and extension of the flexible regions. In this context, using the program BUNCH one starts with a known crystallographic structure which is divided in rigid domains connected by ”dummy residues” chains.[35] The dummy residues represent protein fragments which are substituted by a flexible chain of interconnected amino acid residues. A simulated annealing protocol is used to find the optimal positions and orientations of the rigid domains and the probable conformations of the dummy residues chains, to simultaneously fit the experimental scattering data. In this procedure, the basic rules of the conformational analysis are fulfilled. For the rigid domains with known structure, the scattering patterns *I(q)* are calculated with the code CRYSOL.[36] The intensities corresponding to the portions with unknown structure represented as dummy residues are calculated using spherical harmonics.

In our case, the fragmentation was performed by dividing each HSA domain into three rigid moieties. The fragments were selected taking into account that the unfolding mechanism maintains intact the 17 sulfur-sulfur bridges.[37] In Figure 1 are visible the rigid and flexible fragments of HSA atomic structure employed in our calculations.[38] The coordinates [PDB entry 2BXG.pdb] were obtained from the Protein Data Bank.[39] To check the results consistency, the agreement between the structures obtained with GA_STRUCT and BUNCH was evaluated. For this purpose, the docking of the 3D structures was done with the program SUPCOMB. From a visual examination and from the calculated overlap goodness factor (NSD), a comparison between the two shapes was made.[40]

2.7 SAXS and DLS data correlation

Starting from the structures obtained with BUNCH and using the HYDROPRO code, the hydrodynamic radii are calculated and compared with those estimated by DLS measurements.[41] The HYDROPRO code computes the hydrodynamic properties of rigid macromolecules starting from an

atomic-level structure, as specified by the atomic coordinates taken from a PDB file supplied by the user. The output gives a proper hydrodynamic model designed by the program itself. The procedure builds a primary hydrodynamic model by replacing non-hydrogen atoms with spherical elements of some fixed radius. The resulting particle, consisting of overlapping spheres, is in turn represented by a shell model treated as described in the work of Carrasco and García de la Torre.[42] The authors suggest an atomic element radius varying in the range of 2-5 Å (we use 3 Å).

3. Results and discussion

The denaturation processes, induced by urea, of the HSA defatted (HSA) and of the albumin completely bound with palmitate (HSAPalm) had been described in another work.[21] A very detailed analysis of SAXS, DLS, CD and fluorescence was carried out. In particular, the SVD analysis and the three-dimensional reconstructions allowed the determination of number, percentage and low resolution structures of the conformers involved in the unfolding process. In this work we compare the data obtained for the HSA urea denaturation process with that obtained for the HSA:ibuprofen system (HSAIbu). It is expected that differences in the opening process can be identified and related to the HSA stability enhancement induced by the drug binding.

3.1 Spectroscopic Data

By increasing the denaturant concentration, in comparison with HSA, both the CD (near-UV and far-UV) and the fluorescence HSAIbu spectra show a delay in the unfolding process. A comparison of the emission intensity values at λ_{em}= 340 nm of the HSAIbu and HSA solutions[21], normalized for the HSA concentration, are shown in Figure 2 together with the wavelength values λ_{max} corresponding to the maximum intensities. The fluorescence intensities of the HSAIbu solutions remain practically unchanged until 3.90 M and then begin to rapidly decrease up to about 6.00 M. In the inset of Figure 2,

the ratio between the HSA (see ref. 21) and HSAIbu fluorescence intensities is reported. From the ratio trends we can observe that a significant static quenching occurs in the case of the HSA in the native form. Indeed, upon binding of the ibuprofen, this static quenching is removed, leading to the observed fluorescence enhancement. Between about 3.00 and 5.50 M urea concentration, the stabilization induced by the ibuprofen gets a noticeable decrease of this ratio, while adding further urea, the differences between the HSAIbu and HSA intensities become negligible. An inspection of the λ_{max} behavior (Figure 2, lower panel) shows that the fluorescence spectra of HSAIbu present an initial blue shift up to about 6.00 M urea and then, a noticeable red shift. Nevertheless, in this case, a direct comparison between HSAIbu and HSA[43] does not show differences, pointing out that the ibuprofen binding has no influence in the spectrum shapes. Generally, the shift of the λ_{max} is due to a polarity variation of the Trp environment. In particular, the red shift is often associated to an increase of the solvent/environment polarity. On the contrary, a hydrophobic surroundings induces a blue shift. Therefore, the final red shift of the HSAIbu spectra highlights a protein unfolding involving a greater exposition of the fluorophores to the solvent. Conversely, the initial blue shift seems to be more difficult to explain. Effectively, many works[44-47] support the "direct interaction mechanism", whereby the urea interacts with the protein backbone, via hydrogen bond, other electrostatic interactions and van der Waals attractions. The direct solvent interactions with the fluorophores can induce important variations in the fluorescence spectra.

The CD data are reported in Figure 3 and 4. In Figure 3 the far-UV and near-UV spectra are shown. In the insets, the ratios MRE_{222}(HSA)/MRE_{222}(HSAIbu) for the far-UV and MRE_{268}(HSA)/MRE_{268}(HSAIbu) for the near-UV data are reported. The ratios for MRE_{268} values point out an ibuprofen stabilization effect in the urea concentration range between 3.00 M and 5.00 M, similarly to the fluorescence spectra ratios. Instead, the values related to the far-UV spectra, indicate a more pronounced stabilization that gets on until about 6.00 M urea. So the secondary structure seems to

obtain a greater stability because of the ibuprofen binding. In Figure 4, the HSAIbu α-helix amount is reported and compared to that of the HSA system. We can note that in the case of the HSAIbu system, the percentage remains unchanged until about 3.90 M and then begins to decrease until 9.00 M urea. Between 3.00 and 5.35 M urea, the CD data reveal the stabilization effect of the bounded anti-inflammatory agent.

3.2 SAXS Data

The SAXS intensities were first directly examined by looking at the $I(q)q^2$ vs. q graphics, known as Kratky plot.[48] In Figure 5, the Kratky plots and the $p(r)$ functions estimated by ITP, relative to the HSAIbu solutions, are shown. The Kratky plot is considered a standard to determine the unfolding process.[28,49,50] The characteristic peak for a native globular protein decreases when partially folded states are present and tends to a typical flat shape for a fully denaturated structure (random coil). The spectra analysis permits to clearly characterize the stabilizing action of the ibuprofen. In particular, the reported curves show that, until about 3.90 M urea there are no significant structural changes. This phenomenon is testified by a first sensitive decrease of the $I(q)q^2$ maximum. Afterwards, the maximum tends to vanish at the highest denaturant concentration, thus indicating that the protein reaches a quite unfolded state.

Some details on the protein structures, as a function of denaturant concentration, can be inferred by inspecting the $p(r)$ functions (Figure 5). Also in this case, we can observe that the first significantly shape changes occur above 3.90 M of urea concentration. Moreover, at the subsequent concentrations, until about 6.00 M urea, the curves preserve the maximum positions and sketch a queue essentially in the final part. Very probably this indicates the presence of at least two conformers: a protein fraction keeps partly a globular structure, as in the closed form, while, as we will see later, a significant fraction of partially open conformers is present (with the SAXS analysis it is possible to reliably detect

conformers present in solution with a fraction > 10%). At higher denaturant concentrations, the *p(r)*'s become quite different with an important shift of both the maximum positions and the D_{max} values.

Some general aspects on the protein unfolding in the HSAIbu system can be inferred from the SAXS results summarized in Table 1. In particular, both the R_g and D_{max} values together with the R_h ones point out that the protein sizes remain almost constant up to a limit value, beyond which there is a gradual expansion. Among the studied denaturant concentrations, the limit value is 3.90 M. This threshold, that we have recognized also in the spectroscopic data analysis, is higher than the ones reported for the defatted HSA (2.50 M urea concentration).[21] This suggests that the presence of the ligand induces a strong stability against the urea denaturation effect. It is interesting to note that at 9.00 M urea the R_g and D_{max} values of HSAIbu are quite smaller than the HSA ones (R_g=70.1 Å and D_{max}=195 Å, see reference 21). This difference of the two unfolding states will be studied in detail with the SVD analysis.

3.3 SVD Analysis

The minimum number of structural states present in the unfolding pathway of the HSAIbu system has been determined by employing the SVD method in the analysis of the $I(q)q^2$ SAXS profiles. In this case the SVD analysis allowed us to distinguish three different states (L=3) performing the study on the complete set of solutions. In particular, by using the equations 3-6, it was possible to obtain the values of the fractional populations of the states $f_N(t)$, $f_{I1}(t)$ and $f_U(t)$ at all urea concentrations (see Figure 6). In the two steps process we can distinguish: a native conformation N (at 0.00 M urea), an intermediate I1 (at 6.05 M urea) and an unfolded structure U (at 9.00 M urea). By means of the $b_{j,I1}$ and the Native, Intermediate and Unfolded fractions at each *t* urea concentration, a good reproduction of the relative Kratky plots, presented in Figure 7, was obtained. By using these fractions it was possible to

extract the MRE_{222}, MRE_{268}, R_g^2, R_h^{-1}, $F340_{280}$ at each urea concentration. In this case the experimental and the calculated values, shown in Figure 8, turned out to be very similar.

The experimental values of MRE_{222}, MRE_{268}, R_g^2, R_h^{-1}, $F340_{280}$ were also analyzed by using the Nick Pace's approach to obtain an estimation of the protein conformational stability. The method had permitted to draw the free energy change in absence of urea ΔG^{H_2O} for the transition N↔I. The free energy value obtained by Muzammil et al.[51] for the HSA N↔I transition is slightly smaller. This suggests that the ibuprofen stabilizes the HSA conformation. The results have been added as supporting information.[52]

The SVD method has also been carried out by introducing the *I(q)* profiles in the A matrix. Within an error of 10%, the resulting *f(t)* fractions are consistent with the analysis performed on the $I(q)q^2$ SAXS profiles (see Figure SI1). However, we exploited the $I(q)q^2$ patterns because conformational variations of molecules with the HSA dimensions, mainly affect the SAXS intensity in the intermediate region ($0.1 < q < 0.2$ Å^{-1}). While a Kratky plot of a globular protein presents a q^2 dependence, the partially or completed unfolded forms show an increase with a q dependence.[28,49] In any case, the SVD analysis allows us to characterize in a good way the three structural shapes present in the investigated urea concentration range. In principle, this method could be also applied to the curves obtained by other techniques (for example CD and fluorescence). In particular, we carried out the SVD analysis by considering the CD data. Although the presence of intermediates could be provided also by the near-UV CD data, in this particular instance, probably due in part to the weak signals, the results had been demonstrated unreliable. As a matter of fact, it had not allowed us to distinguish the presence of three states, but a single step denaturation process was pointed out in the complete urea range (data not shown). The same result was achieved by analyzing the far-UV CD data, that provide information about the changes in the protein secondary structure (data not shown).

The SVD results confirm that the CD data are less diagnostic than the SAXS ones. In fact, a single step process can be excluded if we compare the $f_N(t)$ function values calculated by applying the

Equation 7 to MRE_{222}, MRE_{268}, R_g^2, R_h^{-1} and $F340_{280}$ (see Figure 9). The different patterns, corresponding to the various experimental data, require the presence of a multistep process during the protein unfolding.

3.4 Three-dimensional restored structures

The *I(q)* patterns obtained with the SVD analysis allowed us to get more detailed information on the structures present in solution at various urea concentrations. Indeed, the opening mechanism can be obtained by analyzing the N, I1 and U relative spectra with the GA_STRUCT and BUNCH codes. The three-dimensional structures calculated with BUNCH are reported in Figure 10. For these three albumin conformers, recovered structures obtained with the GA_STRUCT program are also drawn together with their superimposition with the BUNCH structures.

In particular, for the protein without denaturant, a structure very similar to the crystallographic heart shape is reported, with only a slight separation of the three domains.[53-55] The structure of the intermediate I1 is instead characterized by only a closed domain (domain III). In detail, the extension of the two open domains gives rise to a maximum particle size of about 145 Å, in a good agreement with the D_{max} obtained from the *p(r)* function. Attempts of BUNCH minimizations keeping closed the domain II or the domain I have been performed. They give rise to calculated patterns with bad agreement indexes, 1.25 and 1.35 times higher, respectively. On the other hand, as shown in Figure 2, the drastic decrease of the $F340_{295}$ at 6.05 M, excludes the presence of a conformer with the domain II closed at this urea concentration.

Finally, the recovered structure representing the Unfolded state at 9.00 M urea reveals the characteristic feature of a completely open state. The presence of an extended conformation is confirmed by an intense growth of the GA_STRUCT volume (407000 $Å^3$ at 9.00 M urea vs. 81000 $Å^3$

at 0.00 M urea). As reported by Heller,[34] it is the evidence of a huge conformational mobility, proper of an unfolded protein in solution.

Comparing these results with the free HSA ones,[21] it is clear that the ibuprofen binding stabilization effect occurs already at low urea concentrations. In the HSAIbu denaturation process, at about 3.00 M of urea, still we note the absence of an intermediate. On the contrary, in the HSA unfolding process, an intermediate which presents the domain I open, has been detected.[21] The HSAIbu complex remains practically in a complete globular form until about 3.90 M urea. Further addition of denaturant leads to a progressive presence of an intermediate I1 with a structure which presents the I and II domains open. Therefore, at 6.05 M the I1 intermediate of the HSAIbu has the same open domains of the second intermediate state, named I2, present in the HSA unfolding pathway. Effectively, there is a good agreement between the SAXS pattern of the HSAIbu solution at urea 6.05 M and that of the HSA solution at urea 5.35 M (see Figure 11). So, if we exchange in the HSA SVD analysis the I2 scattering profile with the HSAIbu solution at urea 6.05 M (it contains 100% of intermediate), we observe there are not significant variations of the HSA SVD results and the population fractions are preserved.

Moreover, in Figure 11 the similarities between these two SAXS intensities are also evidenced by reporting a superimposition of the two structures obtained by applying the BUNCH analysis. This can be considered a further confirmation that the presence of ibuprofen does not change dramatically the unfolding HSA mechanism, but it provokes a shift of the equilibrium towards higher urea concentrations. As a matter of fact, at higher urea concentrations, a fraction of the HSAIbu begins to be completely open. From the urea concentration of 7.60 M, only an unfolded protein structure is present in solution. Worthy of note is the fact that also at 9.00 M of urea, even if the three domains are opened, the dimensional parameters are lower than in the case of HSA without ligand. This is confirmed if we introduce in the HSAIbu SVD analysis also the HSA at 9.00 M urea as Unfolded state. We obtain a good fit considering again only three states and the same fraction of N and I1 until the I1 intermediate

(that corresponds even in this case with the solution at 6.05 M of urea). For the higher urea concentrations, the fractions differ from the previous up to a maximum of 0.2. In particular, the HSAIbu solutions at urea 7.60 and 9.00 M contain 80% of the U conformation.

So we can conclude that the conformation of the HSAIbu at urea 9.00 M, that we defined as the Unfolded state, actually is less expanded. Therefore, as we put in evidence for the HSA-palmitic acid complex, the presence of the ligand seems to stabilize the protein also at very high urea concentrations.[21]

3.5 Comparison between SAXS and DLS

DLS measurements allow us to observe the effect of the denaturation induced by urea monitoring the increase of the hydrodynamic radius with the urea addition. The hydrodynamic radii are summarized in Table 1. In the samples without denaturant, the values of HSA do not show significant changes when the ibuprofen is added, and an R_h value, in agreement with that reported in literature for free albumins, is observed.[45,53,54] Starting from this value, by increasing the denaturant concentration, an increment of the protein size is observed.

A stabilizing effect is shown by the interaction of the albumins with ibuprofen. As a matter of fact, the increase of the R_h values for the samples in presence of the anti-inflammatory drug is smoother than in the corresponding free of drug ones. Moreover, R_h values for the protein-ibuprofen complexes almost equal to the native protein value are preserved up to about 5.00 M denaturant. By means of the structures obtained with BUNCH and by using the HYDROPRO code,[41] the hydrodynamic radii have been calculated for each conformer. In particular, the calculated R_h values are 37.0, 46.5 and 54.0 ± 1.5 Å for the N, I1 and U HSAIbu forms, respectively. Taking into account the composition determined with the SVD method (Figure 6), the hydrodynamic radius in each sample R_{hc} was estimated as a

function of the hydrodynamic radii of the conformers R_{hi} and the corresponding fractions in the sample f_i, as[56]

$$R_h = \left(\sum_i f_i R_{hi}^{-1} \right)^{-1} \quad (8)$$

and compared with the experimental ones in Figure 12. At higher urea concentrations some differences are detected between the experimental and the calculated R_h. These inconsistencies are probably due to an error in the experimental data which is determined by a difficulty in separating the protein and the solvent contributions to the scattering intensity autocorrelation function.

4. Conclusions

Many spectroscopic studies were undertaken to identify the albumin unfolding pathways in chemical denaturant conditions and the increasing stability induced by the presence of exogenous and endogenous compounds. Studies on the stabilization induced by different chemical agents are of considerable importance.[14-17,21,57-59] We performed a study on the stabilization effect of a NSAID, the ibuprofen. To verify the protective action of the ibuprofen, an analysis with SAXS, DLS, CD and fluorescence techniques was carried out on a set of solutions with urea concentrations between 0.00 and 9.00 M.

By comparing the interpretation of the spectroscopic and the scattering data of the HSAIbu system with the results obtained for the free HSA defatted solutions[21] it was clear that in the case of the HSAIbu, the unfolding process takes place later on the denaturant concentration scale. Indeed, we observed that the HSA binding ibuprofen molecules remained in the native form up to a limit urea concentration of 3.90 M. This limit value is higher than the one reported for HSA (2.50 M). This was confirmed also by the analysis performed with the SVD method, applied both to the $I(q)q^2$ and $I(q)$

SAXS profiles. It allowed us to point out that the HSAIbu opening is a two step process involving a native N (at 0.00 M urea), an intermediate I1 (at 6.05 M urea) and an unfolded U (at 9.00 M urea) state, and to get their low resolution structures. It was not observable an intermediate with only the domain I open, that was present in the beginning of the HSA unfolding process, at about 3.00 M of urea.

This result could be questionable in view of the fact that the two ibuprofen specific binding sites involve, in order of binding constants, the domains III and II,[20] and not the domain I. However, at our HSA:Ibu ratio (1:10) other molecules could have a cooperative effect inducing the stabilization of the domain I up to higher urea concentrations than in the case of defatted albumin.

The HSAIbu remained practically in a complete globular form until about 3.90 M urea. We could hypothesize that the presence of the specific ligands did not change drammatically the unfolding mechanism in urea, but it provoked a significant shift of the equilibrium towards higher urea concentrations. This hypothesis was confirmed by both *ab initio* and rigid body fitting methods, which highlighted a stepwise evolution of the protein structure toward open conformations. The greater instability of the domain I was in agreement with the hypothesis of a “direct interaction mechanism” whereby the urea interacted directly with the protein backbone. As a matter of fact, the HSA is characterized by a gradient of charge from the I to the III domain, so the bigger presence of charged or polar residues in the I domain made it more subjected to the electrostatic interactions with the urea by the hydrogen bonds formation. Also in a recent work of Chen et al., even if in this case a “direct interaction mechanism” was not accepted, it was reported that the urea molecules affect the hydrogen bonding of interfacial water molecules, altering in this way, the solvation of the proteins. A visualization of the different interaction between the bovine serum albumin and the urea by changing the protein charge surface was reported.[60]

Finally, the SAXS technique, supported by light scattering measurements and spectroscopic data allowed us to restore the 3D structure at low resolution and to visualize the unfolding mechanism also in presence of a ligand.

This study not only suggests that the HSA stability is enhanced upon binding with the NSAID molecules, but adds information of a structural nature on the mechanism of stabilisation. Note that the study of the ligand effect on the conformational stability of HSA, as well as the determination of the urea-induced unfolding pathway, necessitate only of the knowledge of the HSA crystallographic structure. By combining the structural reconstruction methods with the SVD analysis, the opening sequence in the presence of the ligand-effect can be determined, giving a low-resolution structure of the intermediates. The results would allow the identification of the ligand binding sites. This type of analysis could be exploited in future investigations on proteins in solution, in the binding of drugs or endogenous compounds and in the pharmacokinetic properties. It could be possible to investigate the modification of the protein structure involved in cobinding mechanisms, discriminating potentially among the different cobinding types: independent, cooperative, anticooperative and competitive.[61]

Acknowledgment.

We thank Prof. W. T. Heller for graciously supplying the GA_STRUCT code. We acknowledge the support of the European Community-Research Infrastructure Action under the FP6 ‘‘Structuring the European Research Area Program contract number RII/CT/2004/5060008’’ to the European Molecular Biology Laboratory (EMBL), Hamburg outstation that covered the travel and accommodation expenses of Claudia Leggio at the EMBL Hamburg. The technical assistance of Mr. Antonio Ulisse was very appreciated. We thank MIUR for the financial support (PRIN project 2006 039789-001) and CASPUR for the Standard HPC Grant 2009 Std09-408.

Supporting Information Available: Text about the Nick Pace's approach used to obtain an estimation of the protein conformational stability, Figure SI1 and its description. This material is available free of charge via the Internet at http://www.sciencedirect.com

References

1. D.S. Goodman, The interaction of human serum in albumin with long-chain fatty acid anions, J. Am. Chem. Soc. 80 (1958) 3892–3898.

2. G. Sudlow, D.J. Birkett, D.N. Wade, The Characterization of Two Specific Drug Binding Sites on Human Serum Albumin, Mol. Pharmacol. 11 (1975) 824-832.

3. G. Sudlow, D.J. Birkett, D.N. Wade, Further Characterization of Specific Drug Binding Sites on Human Serum Albumin, Mol. Pharmacol. 12 (1976) 1052-1061.

4. I. Sjöholm, B. Ekman, A. Kober, I. Ljungstedt-Pahlman, B. Seiving, T. Sjodin, Binding of drugs to human serum albumins, Mol. Pharmacol. 16 (1979) 767-777.

5. N.P. Sollene, G.E. Means, Characterization of a specific drug binding site of human serum albumin. Means. Characterization of a specific drug binding site of human serum albumin, Mol. Pharmacol. 14 (1979) 754-757.

6. Y. Ozeki, Y. Kurono, T. Yotsuyanagi, K. Ikeda, Effects of drug binding on the esterase activity of human serum albumin: inhibition modes and binding sites of anionic drugs, Chem. Pharmac. Bull. 28 (1980) 535-540.

7. Y. Kurono, Y. Ozeki, H. Yamada, T. Takeuchi, K. Ikeda, Effects of drug bindings on the esterase-like activity of human serum albumin. VII. Subdivision of R-type drugs inhibiting the activity towards *p*-nitrophenyl acetate, Chem. Pharmac. Bull. 35 (1987) 734-739.

8. U. Kragh-Hansen, Relations between high-affinity binding sites for L-tryptophan, diazepam, salicylate and Phenol Red on human serum albumin, Biochem. J. 209 (1983) 135-142.

9. U. Kragh-Hansen, Relations between high-affinity binding sites of markers for binding regions on human serum albumin, Biochem. J. 225 (1985) 629-638.

10. U. Kragh-Hansen, Evidence for a large and flexible region of human serum albumin possessing high affinity binding sites for salicylate, warfarin, and other ligands, Mol. Pharmacol. 34 (1988) 160-171.

11. K. Yamasaki, T. Maruyama, U. Kragh-Hansen, M. Otagiri, Characterization of site I on human serum albumin: concept about the structure of a drug binding site, Biochim. Biophys. Acta 1295 (1996) 147-157.

12. T. Itoh, Y. Suara, Y. Tsuda, H. Yamada, Stereoselectivity and enantiomer-enantiomer interactions in the binding of ibuprofen to human serum albumin, Chirality 9 (1997) 643-649.

13. L. Jin, D.Y. Choi, H. Liu, R.H. Row Protein binding study of S-ibuprofen using high-performance frontal analysis, Bull. Korean Chem. Soc. 26 (2005) 136-138.

14. F.P. Nicoletti, , B.D. Howes, M. Fittipaldi, G. Fanali, M. Fasano, P. Ascenzi, G. Smulevich, Ibuprofen Induces an Allosteric Conformational Transition in the Heme Complex of Human Serum Albumin with Significant Effects on Heme Ligation, J. Am. Chem. Soc. 130 (2008) 11677-11688.

15. L. Saso, B. Silvestrini, I. Zwain, A. Guglielmotti, M.R. Luparini, V. Cioli, C.Y. Cheng, Abnormal glycosylation of hemopexin in arthritic rats can be blocked by bindarit, J. Rheumatol. 19 (1992) 1859-1867.

16. L. Saso, G. Valentini, M. L. Casini, E. Mattei, L. Braghiroli, G. Mazzanti, C. Panzironi, E. Grippa and B. Silvestrini, Inhibition of Protein Denaturation by Fatty Acids, Bile Salts and Other Natural Substances: A New Hypothesis for the Mechanism of Action of Fish Oil in Rheumatic Diseases, Jpn J Pharmacol. 79 (1999) 89-99.

17. G. Fanali, P. Ascenzi, M. Fasano, Effect of prototypic drugs ibuprofen and warfarin on global chaotropic unfolding of human serum heme-albumin: A fast-field-cycling ^{1}H-NMR relaxometric study, Biophys. Chem. 129 (2007) 29-35.

18. M.K. Santra, A. Banerjee, O. Rahaman, D. Panda, Unfolding pathways of human serum albumin: Evidence for sequential unfolding and folding of its three domains, Int. J. Biol. Macro. 37 (2005) 200-204.

19. M. Rezaei-Tavirani, S.H. Moghaddamnia, B. Ranjbar, M. Amani, S.A. Marashi, Conformational Study of Human Serum Albumin in Pre-denaturation Temperatures by Differential Scanning Calorimetry, Circular Dichroism and UV Spectroscopy, J. Biochem. Mol. Biol. 39 (2006) 530-536.

20. J. Ghuman, P.A. Zunszain, I. Petipas, A.A. Bhattacharya, M. Otagiri, S. Curry, Structural basis of the drug-binding specificity of human serum albumin, J. Mol. Biol. 353 (2005) 38-52.

21. C. Leggio, L. Galantini, P. V. Konarev and N. V. Pavel, Urea-Induced Denaturation Process on Defatted Human Serum Albumin and in the Presence of Palmitic Acid, J. Phys. Chem. B 113 (2009) 12590-12602.

22. C.N. Pace, F. Vajdos, L. Fee, G. Grimsley, T. Gray, How to measure and predict the molar absorption coefficient of a protein, Protein Sci. 4 (1995) 2411-2423.

23. Y.H. Chen, J.T. Yang, H.M. Martinez, Determination of the secondary structures of proteins by circular dichroism and optical rotatory dispersion, Biochemistry 11 (1972) 4120-4131.

24. M.W. Roessle, R. Klaering, U. Ristau, B. Robrahn, D. Jahn, T. Gehrmann, P.V. Konarev, A. Round, S. Fiedler, C. Hermesand, D. I. Svergun, Upgrade of the small-angle x-ray scattering beamline X33 at the European Molecular Biology Laboratory, Hamburg, J. Appl. Crystallogr. 40 (2007) s190–s194.

25. P.V. Konarev, M.V. Petoukhov, V.V. Volkov, D.I. Svergun, *ATSAS* 2.1, a program package for small-angle scattering data analysis, J. Appl. Crystallogr. 39 (2006) 277–286.

26. P.V. Konarev, V.V. Volkov, A.V. Sokolova, M.H.J. Koch, D.I. Svergun, PRIMUS: a Windows PC-based system for small-angle scattering data analysis, J. Appl. Crystallogr. 36 (2003) 1277-1282.

27. H. Stabinger, O. Kratky, A. New Technique for the Measurement of the Absolute Intensity of X-Ray Small Angle Scattering, The Moving Slit Method, Makromol. Chem. 179 (1978) 1655-1659.

28. O. Glatter, Small Angle X-ray Scattering (Academic Press, London, 1982).

29. D. Orthaber, A. Bergmann, O. Glatter, SAXS experiments on absolute scale with Kratky systems using water as a secondary standard, J. Appl. Crystallogr. 33 (2000) 218-225.

30. O. Glatter, A new method for the evaluation of small-angle scattering data, J. Appl. Crystallogr. 10 (1977) 415-421.

31. W.H. Press, B.P. Flannery, S.A. Teukolsky, W.T. Vatterling, Numerical Recipes: The Art of Scientific Computing (Cambridge University Press, New York, 1989).

32. L. Chen, K.O. Hodgson, S. Doniach, A lysozyme folding intermediate revealed by solution x-ray scattering, J. Mol. Biol. 261 (1996) 658-671.

33. W.T. Heller, J.K. Krueger, J. Trewhella, Further insights into calmodulin-myosin light chain kinase interaction from solution scattering and shape restoration, Biochemistry 42 (2003) 10579-10588.

34. W.T. Heller, Influence of multiple well defined conformations on small-angle scattering of proteins in solution, Acta Crystallogr. *D61* (2005) 33-44.

35. M.V. Petoukhov, D.I. Svergun, Global Rigid Body Modeling of Macromolecular Complexes against Small-Angle Scattering Data, Biophys. J. 89 (2005) 1237-1250.

36. D.I. Svergun, C. Barberato, M.H.J. Koch, *CRYSOL* - a Program to Evaluate X-ray Solution Scattering of Biological Macromolecules from Atomic Coordinates, J. Appl. Crystallogr. 28 (1995) 768-773.

37. K. Takeda and Y. Moriyama, Comment on the misunderstanding of the BSA-SDS complex model: concern about publications of an impractical model, J. Phys. Chem. B. 111 (2007) 1244.

38. J. Ghuman, P.A. Zunszain, I. Petitpas, A.A. Bhattacharya, M. Otagiri, S. Curry, Structural basis of the drug-binding specificity of human serum albumin, J. Mol. Biol. 353 (2005) 38-52.

39. H.M. Berman, J. Westbrook, Z. Feng, G. Gilliland, T.N. Bhat, H. Weissig, I.N. Shindyalov, P.E. Bourne, The Protein Data Bank, Nucleic Acids Res. 28 (2000) 235-242.

40. M.B. Kozin, D.I. Svergun, A software system for rigid body modeling of solution scattering data, J. Appl. Crystallogr. 34 (2001) 33-41.

41. J. García de la Torre, M.L. Huertas, B. Carrasco, Calculation of Hydrodynamic Properties of Globular Proteins from Their Atomic-Level Structure, Biophys. J. 78 (2000) 719-730.

42. B. Carrasco, J. García de la Torre, Hydrodynamic Properties of Rigid Particles: Comparison of Different Modeling and Computational Procedures, Biophys. J. 76 (1999) 3044-3057.

43. J. González-Jiménez, M. Cortijo, Urea-Induced Denaturation of Human Serum Albumin Labeled with Acrylodan, J Prot. Chem. 21 (2002) 75-79.

44. R. Itri, W. Caetano, L.R.S. Barbosa, M.S. Baptista, Effect of Urea on Bovine Serum Albumin in Aqueous and Reverse Micelle Environments Investigated by Small Angle X-Ray Scattering, Fluorescence and Circular Dichroism, Braz. J. Phys. 34 (2004) 58-63.

45. A. Caballero-Herrera, K. Nordstrand, K.D. Bernt, L. Nilsson, Effect of urea on peptide conformation in water: molecular dynamics and experimental characterization, Biophys. J. 89 (2005) 842-857.

46. L.J. Smith, R.M. Jones, W.F. Gunsteren, Characterization of the denaturation of human α-lactalbumin in urea by molecular dynamics simulations, Proteins 58 (2005) 439-449.

47. L. Hua, R. Zhou, D. Thirumalai, B.J. Berne, Urea denaturation by stronger dispersion interactions with proteins than water implies a 2-stage unfolding, Proc. Natl. Acad. Sci. 105 (2008) 16928-16933.

48. O. Kratky, I. Pilz, A comparison of X-ray small-angle scattering results to crystal structure analysis and other physical techniques in the field of biological macromolecules, *Q. Re*V. *Biophys.* 5 (1972) 481-537.

49. D.J. Segel, A.L. Fink, K.O. Hodgson, S. Doniach, A small-angle X-ray scattering study of the ensemble of unfolded states of cytochrome *c,* Biochemistry 37 (1998) 12443-12451.

50. D.J. Segel, A. Bachmann, J. Hofrichter, K.O. Hodgson, S. Doniach, T. Kiefhaber, Characterization of transient intermediates in lysozyme folding with time-resolved small-angle X-ray scattering, J. Mol. Biol. 288 (1999) 489-499.

51. S. Muzammil, Y. Kumar, S. Tayyab, Anion-induced stabilization of human serum albumin prevents the formation of intermediate during denaturation, Proteins 40 (2000) 29-38

52. C.N. Pace, Denaturation and analysis of urea and guanidine hydrochloride denaturation curves, Methods Enzymol. 131 (1986) 266-279.

53. C. Leggio, L. Galantini, N.V. Pavel, About the albumin structure in solution: cigar Expanded form versus heart Normal shape, Phys. Chem. Chem. Phys. 10 (2008) 6741-6750.

54. L. Galantini, C. Leggio, N.V. Pavel, Human Serum Albumin Unfolding: A Small-Angle X-ray Scattering and Light Scattering Study, J. Phys. Chem. B 112 (2008) 15460-15469.

55. F. Zhang, M.W.A. Skoda, R.M.J. Jacobs, R.A. Martin, C.M. Martin, F. Schreiber, Protein Interactions Studied by SAXS: Effect of Ionic Strength and Protein Concentration for BSA in Aqueous Solutions, J. Phys. Chem. B 111 (2007) 251-259.

56. A.A. D'Archivio, L. Galantini, E. Tettamanti, Study on Intermicellar Interactions and Micellar Size in Aqueous Solutions of NaTDC by Measurements of Collective Diffusion and Self-Diffusion Coefficients, J. Phys. Chem. B, 104 (2000) 9255-9259.

57. A. Sulkowska, B. Bojko, J. Rownicka, D. Pentak, W. Sulkowski, Effect of urea on serum albumin complex with antithyroid drugs: fluorescence study, J. Mol. Struct. 651 (2003) 237.

58. A. Chakrabarty, A. Mallick, B. Haldar, P. Das, N. Chattopadhyay, Binding Interaction of a Biological Photosensitizer with Serum Albumins: A Biophysical Study, *Biomacromolecules* 8 (2007) 920-927.

59. M.A. Cheema, P. Taboada, S. Barbosa, J. Juarez, M. Gutierrez-Pichel, M. Siddiq, V. Mosquera, Human serum albumin unfolding pathway upon drug binding: A thermodynamic and spectroscopic description, J. Chem. Thermodynamics 41 (2009) 439-447.

60. X. Chen X, L.B. Sagle, P.S. Cremer, Urea orientation at protein surfaces, J. Am. Chem. Soc. 129 (2007) 15104-15105.

61. G. Ascoli, C. Bertucci, P. Salvadori, Stereospecific and competitive binding of drugs to human serum albumin: a difference circular dichroism approach, J. Pharm. Sci. 84 (1995) 737-41.

Figure Captions

Figure 1 On the top, amino acid sequence of HSA in an arrangement reflecting the heart-shaped structure. The I–III domains are shown, respectively, in blue, green and red. The grey spheres indicate the amino acids that have been considered as dummy residues in the BUNCH calculations. The amino acids that in the crystallographic structure are nearer than 7 Å to the ibuprofen molecules are also marked in magenta and cyan. On the bottom, a 3D representation of the HSA structure and the rigid and flexible fragments used in the BUNCH calculations. Nine loops (three for each domain) are held together by 17 disulphide bridges. In cyan and magenta the two binding sites of the ibuprofen are evidenced. This is the view with the program PyMOL. PyMOL is a trademark of DeLano Scientific LLC.

Figure 2. In the upper panel, fluorescence intensity monitored at λ_{em}= 340 nm corresponding to λ_{ex}= 295 nm for HSAIbu (open circle) and for HSA (cross) solutions at various urea concentrations. In the insets, the ratio HSA/HSAIbu of $F340_{295}$ are reported. In the lower panel, relative λ_{max} versus urea concentration are shown. In the insets the ratio HSA/HSAIbu of λ_{max} are reported.

Figure 3. Far-UV spectra (top) and near-UV spectra (bottom) relative to HSAIbu solutions at various urea concentrations. In the insets, the values of the ratio HSA/HSAIbu of MRE_{222} (top) and MRE_{268} (bottom) are reported.

Figure 4. Amount of α-helix relative to HSA (square) and HSAIbu (circle) for increasing urea concentration.

Figure 5. Pair distribution functions *p(r)* of HSAIbu (top) and the relative Kratky plots (bottom) at various urea concentrations.

Figure 6. The fractional populations $f_N(t)$ (open circle), $f_{I1}(t)$ (square) and $f_U(t)$ (diamond) estimated by the SVD analysis (by using the Equations 4-6) for the HSAIbu at all urea concentrations.

Figure 7. Kratky plots relative to HSAIbu at various urea concentrations. The functions calculated with the SVD method are represented with dash lines**.**

Figure 8. From the top: values of gyration radii (by the SAXS spectra), hydrodynamic radii (by DLS), fluorescence intensity (λ_{ex}= 280 nm, λ_{em}= 340 nm), MRE at 222 nm (by far-UV CD), MRE at 268 nm (by near-UV CD), for HSAIbu solutions at different urea concentrations. The experimental data (circle) are compared with the calculated ones (square), obtained by means of the SVD analysis. R_g and R_h are expressed in Å, MRE_{222} and MRE_{268} are expressed in 10^{-3} deg cm^2 mol^{-1} and deg cm^2 mol^{-1}, respectively.

Figure 9. $f_N(t)$ functions (calculated by applying the Equation 7) for MRE_{222} and MRE_{268}, R_g^2, R_h^{-1} and $F340_{280}$, of the HSAIbu solutions at various urea concentrations.

Figure 10. Three dimensional structures obtained for the HSAIbu with the BUNCH code, GA_STRUCT consensus envelopes, and their superimpositions. The three HSA domains are in blue, green and red, respectively. Two orthogonal viewpoints are reported. The structures refer to the three configurations that evolve in solution increasing the urea concentration. On the right the summarizing schematization of the relative opening mechanisms is reported.

Figure 11. On the left: three dimensional structures obtained by BUNCH for the HSA solution at urea 5.35 M (top) and the HSAIbu one at urea 6.05 M (bottom). On the right: two orthogonal viewpoints of the superimposed structures. In red the HSA solution at urea 5.35 M and in blue the HSAIbu one at urea 6.05 M. In the lower panel the $p(r)$ (left) and the $I(q)$ (right) curves are reported for the HSA (line)

and the HSAIbu (dash line) solutions. For the pair distribution functions only some error bars are reported.

Figure 12. Hydrodynamic radii measured by DLS and estimated from the SAXS conformer distribution for HSAIbu (circles and squares, respectively). The errors of the DLS data are between ± 1 Å (0.00 M urea) and ± 5 Å (9.00 M urea) the error of the radii estimated from SAXS analysis is about 5%.

Figure Captions of the black and white version (in the print) of the Figures 1, 5, 7, 10, 11

Figure 1. Amino acid sequence of HSA in an arrangement reflecting the heart-shaped structure (top). 3D representation of the HSA structure and the rigid and flexible fragments used in the BUNCH calculations. Nine loops (three for each domain) are held together by 17 disulphide bridges. With a circles the two binding sites of the ibuprofen are evidenced. This is the view with the program PyMOL. PyMOL is a trademark of DeLano Scientific LLC (bottom).

Figure 5. Pair distribution functions *p(r)* of HSAIbu (top) and the relative Kratky plots (bottom). The arrows represent the trend increasing the urea concentration.

Figure 7. Kratky plots relative to HSAIbu at various urea concentrations. The functions calculated with the SVD method are represented with dash lines**.** The arrows represent the trend increasing the urea concentration.

Figure 10. Three dimensional structures obtained for the HSAIbu with the BUNCH code, GA_STRUCTconsensus envelopes, and their superimpositions. Two orthogonal viewpoints are reported. Thestructures refer to the three configurations that evolve in solution increasing the urea concentration. On the right the summarizing schematization of the relative opening mechanisms is reported.

Figure 11. On the left: three dimensional structures obtained by BUNCH for the HSA solution at urea 5.35 M (top) and the HSAIbu one at urea 6.05 M (bottom). On the right: two orthogonal viewpoints of the superimposed structures. In the lower panel the *p(r)* (left) and the *I(q)* (right) curves are reported for the HSA (line) and the HSAIbu (dash line) solutions. For the pair distribution functions only some error bars are reported.

T**able**

Table 1. Radius of gyration R_g, hydrodynamic radius R_h and maximum distance D_{max} (expressed in Å) of the HSAIbu at different urea concentrations.

Urea (M)	R_g	R_h	D_{max}
0.00	31.1	36.5	85.
1.80	32.5	36.1	85.
3.00	35.0	36.0	100.
3.90	33.0	38.3	100.
4.35	37.0	39.0	120.
4.80	43.0	39.2	135.
5.35	42.5	41.8	130.
6.05	48.6	50.0	150.
6.65	51.9	52.2	140.
7.60	58.8	56.0	160.
9.00	58.7	58.0	170.

The experimental errors for R_g, R_h and D_{max} are from 1% to 3%, 3% and 5% respectively.

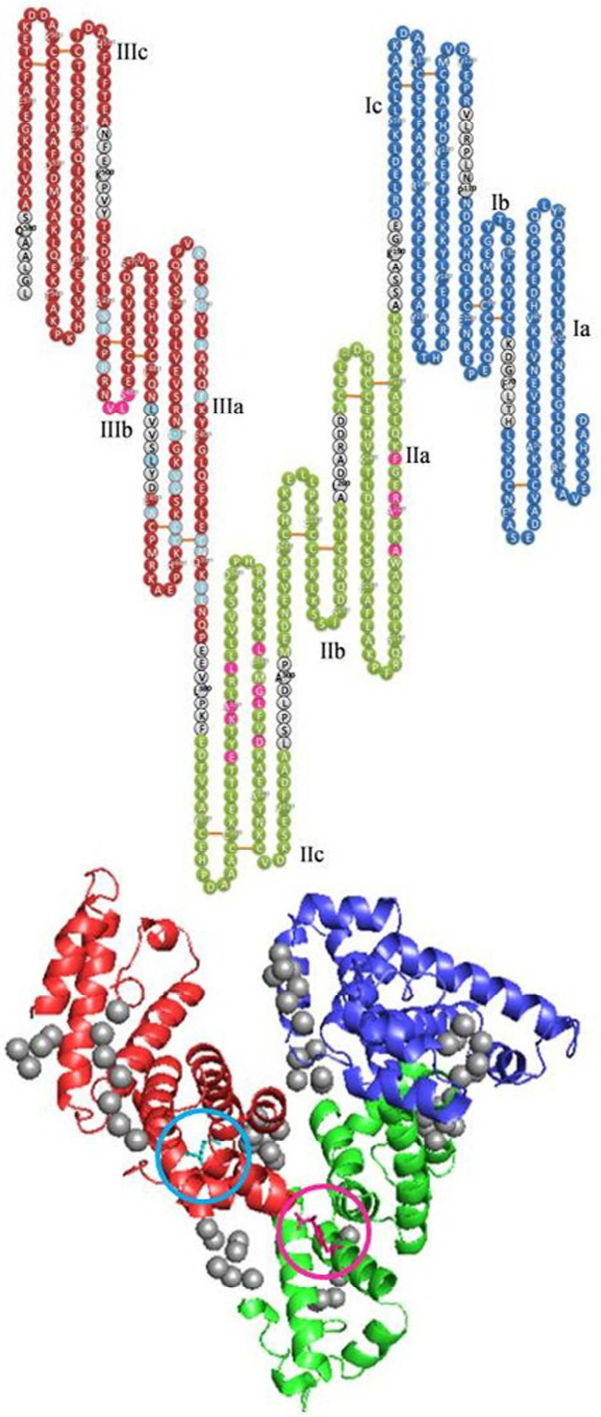

Fig. 1

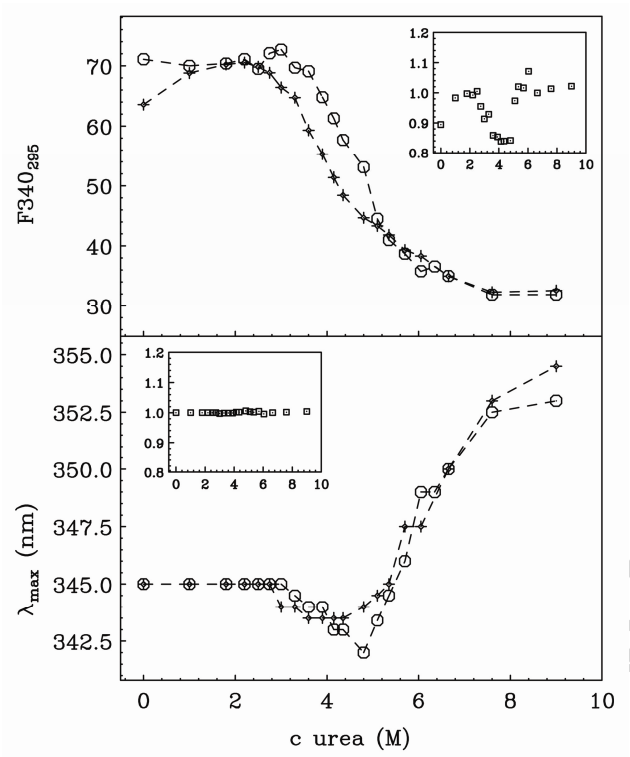

Fig. 2

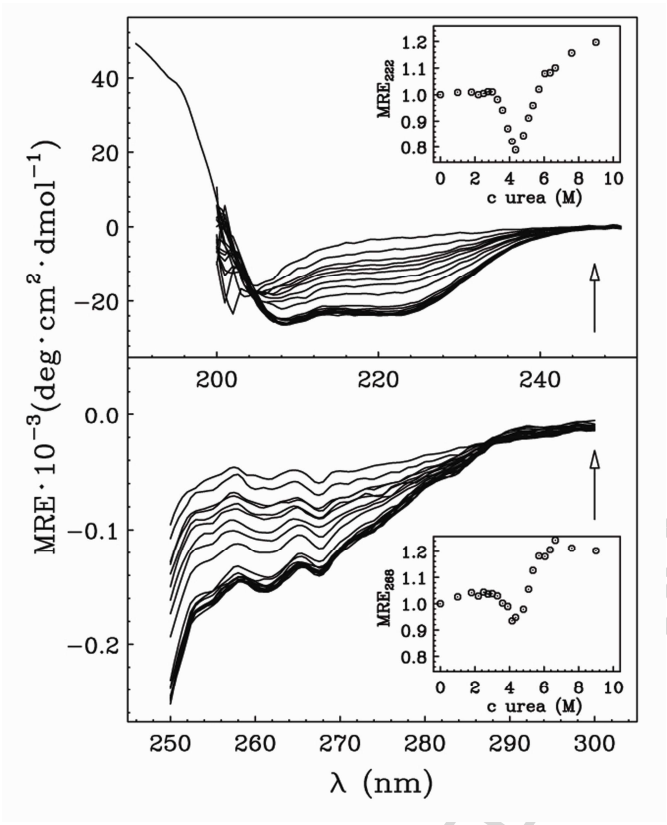

Fig. 3

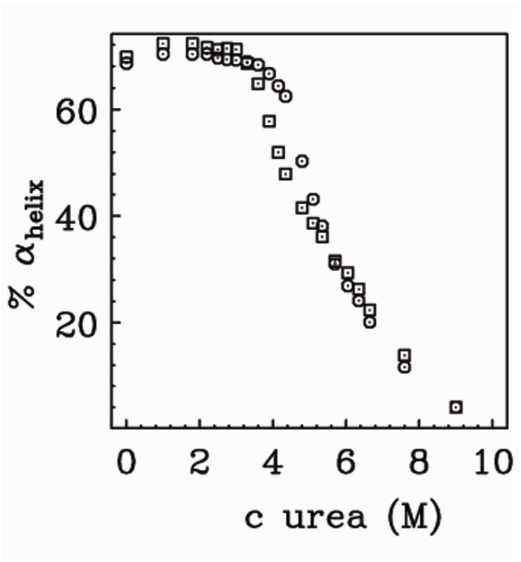

Fig. 4

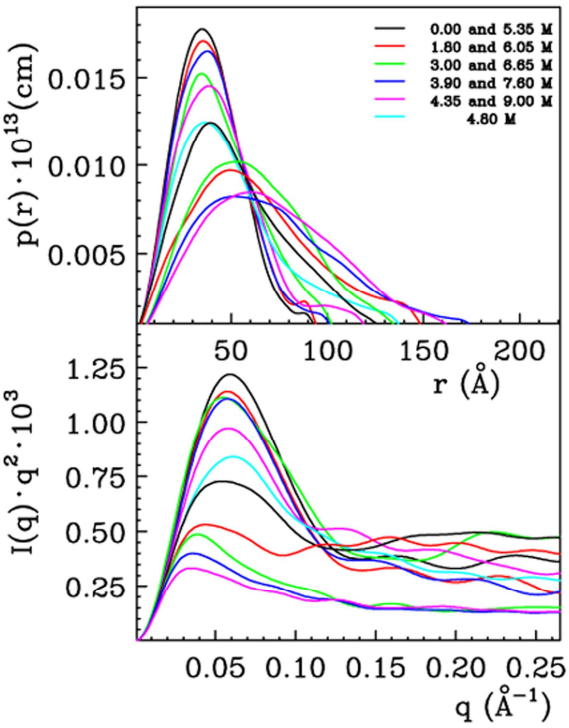

Fig. 5

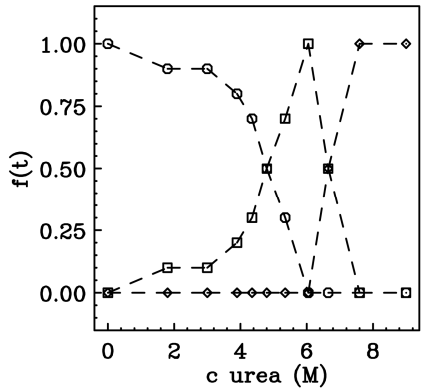

Fig. 6

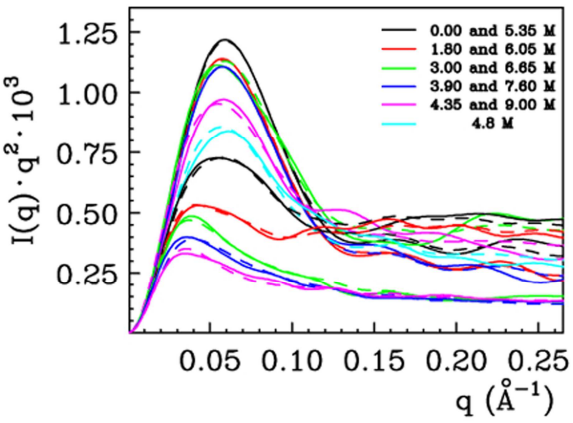

Fig. 7

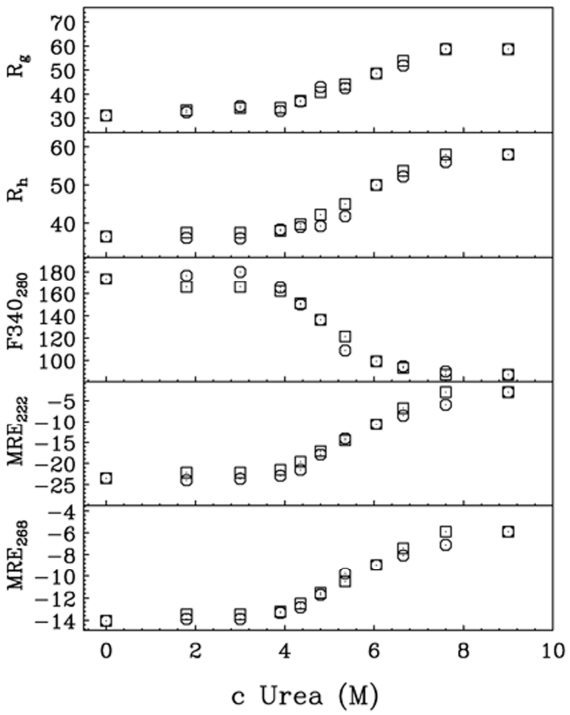

Fig. 8

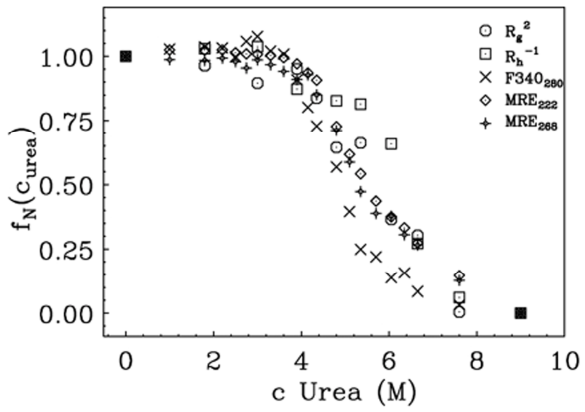

Fig. 9

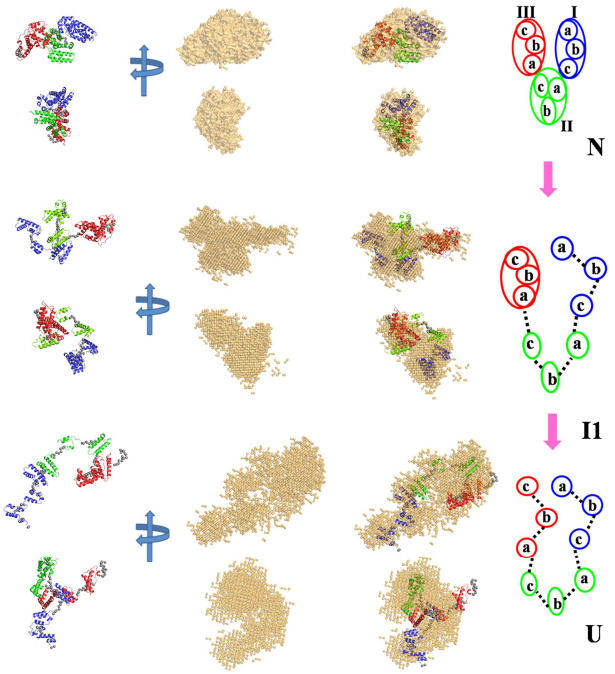

Fig. 10

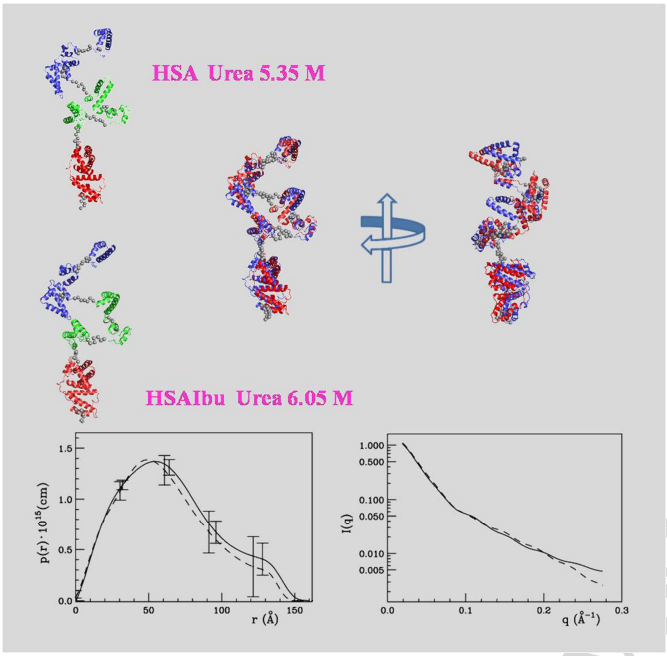

Fig. 11

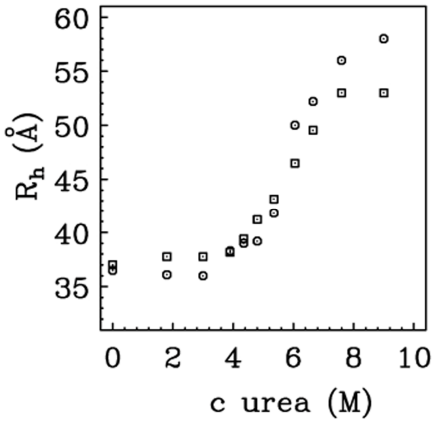

Fig. 12